

LA-UR-16-26317

Approved for public release; distribution is unlimited.

Verification test of the SURF and SURFplus models in xRage: Part III affect of mesh alignment Title:

Author(s): Menikoff, Ralph

Intended for: Report

Issued: 2016-08-17



VERIFICATION TEST OF THE SURF AND SURFPLUS MODELS IN XRAGE: PART III AFFECT OF MESH ALIGNMENT

RALPH MENIKOFF

August 15, 2016

Abstract

The previous studies used an underdriven detonation wave in 1-dimension (steady ZND reaction zone profile followed by a scale-invariant rarefaction wave) for PBX 9502 as a verification test of the implementation of the SURF and SURFplus models in the xRage code. Since the SURF rate is a function of the lead shock pressure, the question arises as to the effect on accuracy of variations in the detected shock pressure due to the alignment of the shock front with the mesh. To study the effect of mesh alignment we simulate a cylindrically diverging detonation wave using a planar 2-D mesh. The leading issue is the magnitude of azimuthal asymmetries in the numerical solution. The 2-D test case does not have an exact analytic solution. To quantify the accuracy, the 2-D solution along rays through the origin are compared to a highly resolved 1-D simulation in cylindrical geometry.

1 Introduction

Previous studies [Menikoff, 2016b,c] used an underdriven detonation wave for PBX 9502 as a verification test of the implementation of the SURF and SURFplus models [Shaw and Menikoff, 2010, Menikoff and Shaw, 2010, 2012] in the xRage code. In 1-D an accurate solution can be determined based on the theoretical structure of the solution; steady ZND reaction zone followed by a scale-invariant rarefaction (known as a Taylor wave), and then a constant state to match the zero velocity boundary condition. This was used to assess the accuracy of the numerical solution. At the finest resolution (cell size of $1\,\mu\rm m$) and away from the sonic point at the end of the reaction zone, the pointwise error in the pressure was a few tenth of per cent in the reaction zone and a hundredth of per cent in the Taylor wave. The error in the lead shock pressure was 0.02 per cent.

An unusual feature of the SURF model is that the burn rate depends on the lead shock pressure. A critical component of the model implementation is an algorithm to detect the lead shock. Shock capturing gives rise to small fluctuations in the detected shock pressure, P_{sh} , which affects the accuracy of the reaction zone. In 2-D, P_{sh} can potentially vary with the alignment of the shock front relative to the computational grid. Here we use a cylindrically diverging detonation wave as a test case. With a planar 2-D mesh, the angle of the shock front varies with respect to the mesh. The azimuthal symmetry of the numerical solution is an important indication of the effect of mesh alignment.

Due to the curvature effect of a propagating detonation wave, a cylindrically diverging detonation wave does not have an analytic solution. Instead, to quantify the accuracy, the 2-D numerical solution along rays through the origin will be compared to a high resolution 1-D simulation in cylindrical geometry.

2 Test problem

The simulations discuss here use the same EOS models for PBX 9502 reactants and products and the same rate parameters as used for the previous studies; see [Menikoff, 2016a, Apps. A-D]. The mesh for the 2-D simulations is the quadrant (0 < x < 100 mm, 0 < y < 100 mm) with reflecting boundary conditions on the left and bottom. It is initialized along rays through the origin with the 1-D underdriven detonation wave used previous, see [Menikoff, 2016c, Figs. 1 and 2 for SURF and SURFplus, respectively]; i.e., $w(x, y) = w_{1D}([x^2 + y^2]^{1/2})$.

Due to the effect of divergence, the reaction zone is only quasi steady and the release wave is not exactly a scale-invariant rarefaction or simple wave. The solution can not be reduced to solving an ODE as in the 1-D case.

2.1 1-D cylindrical simulations

In place of an exact solution, we use the solution of a high resolution (uniform mesh with 1 micron cells) 1-D cylindrical simulation to compare with the 2-D solution along rays through the origin. At this resolution, there is about 200 cells in the SURF reaction zone. The simulations propagate the detonation front from $r = 10 \,\mathrm{mm}$ out to $100 \,\mathrm{mm}$, which takes slightly over $11.5 \,\mu\mathrm{s}$.

For both the SURF and SURFplus models, the evolution of pressure profiles is shown in fig. 1, and the detected lead shock pressure is shown in fig. 2. Due to divergence, the detonation speed is less than the planar CJ value used for the initial profile at t=0. Consequently, there is an initial transient in which the shock pressure drops. Subsequently, the shock pressure increases as

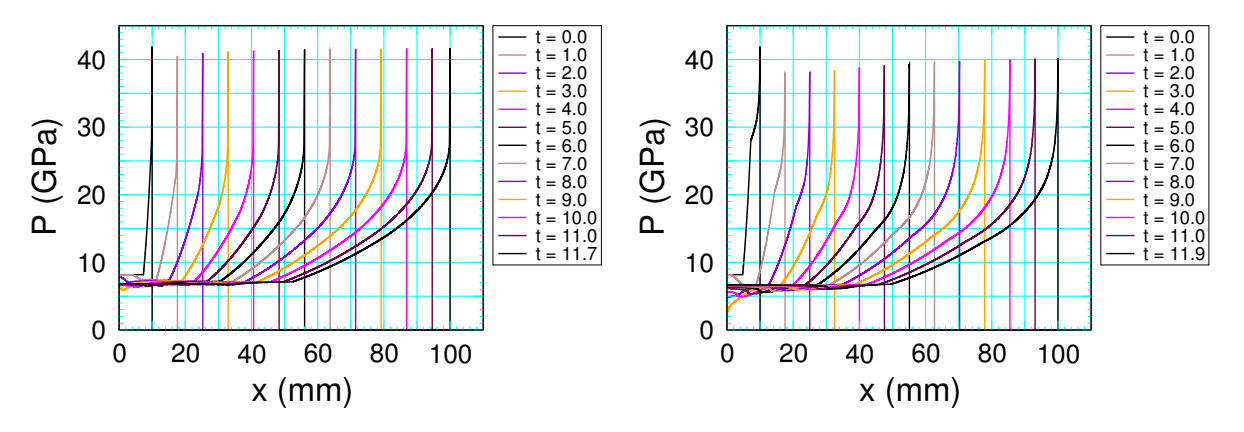


Figure 1: Time evolution of pressure profiles for high resolution 1-D cylindrical simulations. Left plot for SURF model and right plot for SURFplus.

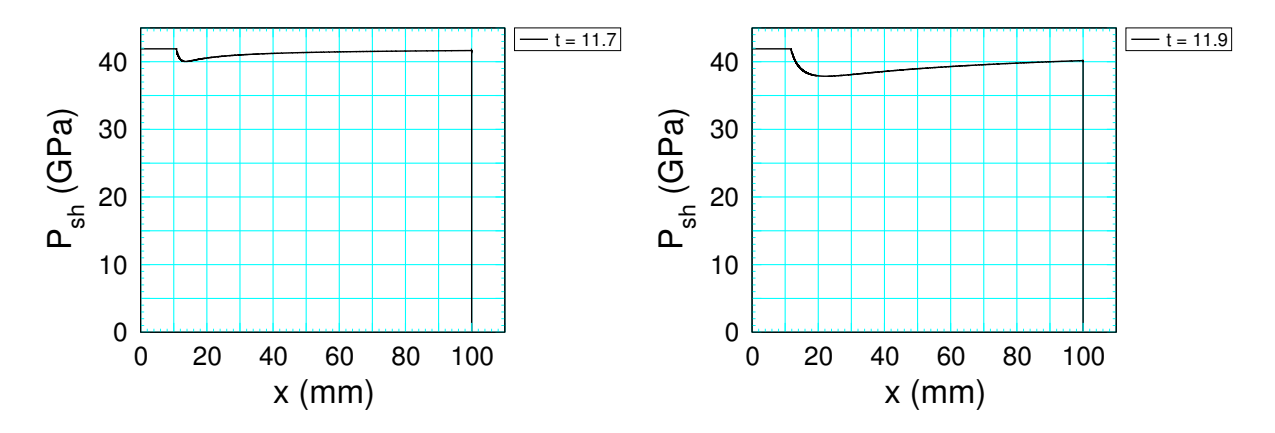


Figure 2: Lead shock pressure (advected) vs distance. Left plot for SURF model and right plot for SURFplus.

the detonation front curvature ($\kappa=1/R$) decreases with radius. Since the reaction zone width of the SURF model is smaller than that of the SURFplus model, the curvature effect is smaller for SURF; *i.e.*, the change in the detonation speed, $D_{CJ}-D(\kappa)$, is smaller for the SURF model, see [Menikoff and Shaw, 2012]. At the end of the run, radius of 100 mm, the lead shock (VN spike) pressure is 41.65 and 40.17 GPa for SURF and SURFplus, respectively. From the reactants EOS, the corresponding detonation speeds are 7.72 and 7.62 km/s, respectively. For a planar detonation wave, the VN spike pressure is 41.9 GPa, the CJ detonation speed is 7.73 km/mm, and CJ pressure is 28.0 GPa. Thus, even at the end of the simulation, the curvature effect is noticeable, but small (a few per cent).

Profiles in the neighborhood of the sonic point at the end of the simulations are shown in fig. 3. For the SURF simulation, the sonic point occurs after the end of the reaction zone rather than slightly before the end as theory predicts. As with the planar case, this is due to smearing of the kink in the pressure profile in the vicinity of the sonic point. In contrast, for the SURFplus model, the sonic point occurs after the fast reaction completes but well before the second reaction is completed; $\lambda_2 \approx 0.3$. In this case, the front curvature has a large effect due to the large reaction zone width of the slow second reaction; see [Menikoff and Shaw, 2012].

The time dependence of the detonation speed and the state at the sonic point, the burning after the sonic point, and the scale set by the radius are major obstacles in obtaining an analytic solution. Due to the variation of the detonation state, the release wave is not exactly isentropic and hence not a simple wave. Moreover, the release wave is not scale invariant. Thus, the key simplifications in planar geometry are no longer valid. Nevertheless, the high resolution solution is sufficiently accurate to use as a comparison for the 2-D planar simulations.

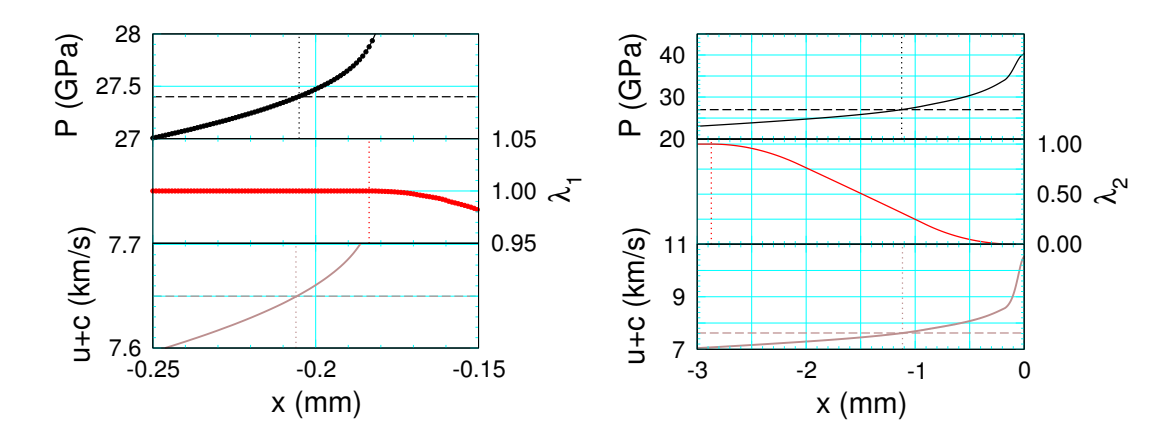


Figure 3: Profiles of pressure, reaction progress variable and characteristic speed (u + c) in neighborhood of sonic point at the end of the simulation (detonation front at $100 \,\mathrm{mm}$). Left plot for SURF model and right plot for SURFplus.

3 Numerical results

For the planar 2-D simulations, a uniform fine grid would be computationally too expensive. Instead an adaptive mesh is used; cell size of 7.8 microns (128 cells per mm) within the fast part of the reaction zone, down to 62.5 microns (16 cells per mm) to resolve the pressure gradient in the slow portion of the reaction zone and in the release wave, and 0.5 mm ahead of the detonation front and behind the tail of the release wave. The fast SURF reaction zone has only about 25 cells.

2-D plots of the detected shock pressure at the end of the simulations, fig. 4, show good azimuthal symmetry with radial variation corresponding to that of the 1-D simulations in fig. 2. Plots of the pressure, fig. 5, show the detonation front is smooth and the overall azimuthal symmetry is good. To quantify the accuracy we next compare the pressure along rays with the high resolution 1-D cylindrically symmetric simulations. We note that the cell size of the 1-D simulations is uniform and 8 times finer than the smallest cells of the 2-D adaptive mesh.

The pointwise error in the pressure profiles along rays for several angles (0 and 90 degrees correspond to the x- and y-axis, respectively) at initialization (t=0) is shown in fig. 6. The profile on a ray is determined by the values of the nearest cell centers and projecting the cell center perpendicular to the ray on to the distance coordinate from the origin, 's'. The interpolation error is less than 0.01 per cent. We note that there is short wave length oscillation due to the cell size and depending on angle. It arises from whether adjacent cell center lie above or below the ray. The amplitude of the error is largest at 45 degress. The pointwise error at complementary angles (θ and $90 - \theta$) is the same.

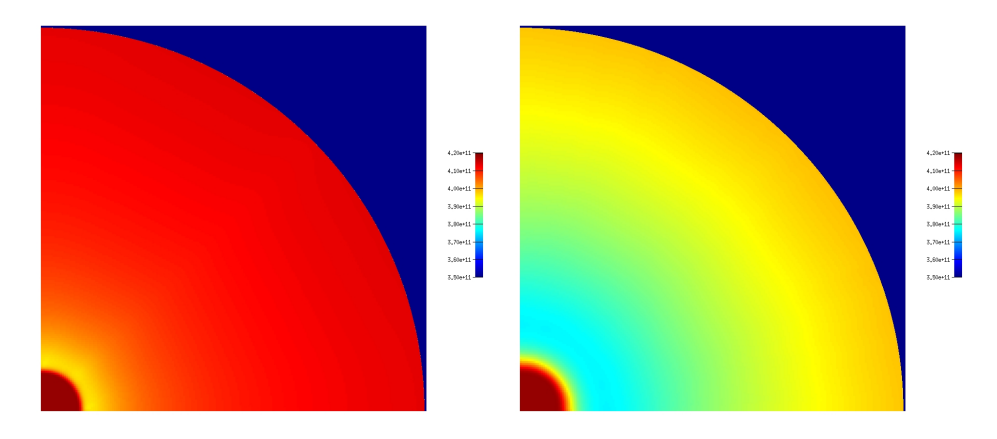


Figure 4: 2-D plots of detected shock pressure (advected) at end of simulations. Left plot for SURF model and right plot for SURFplus. Linear scale from 35 (blue) to 42 (red) GPa.

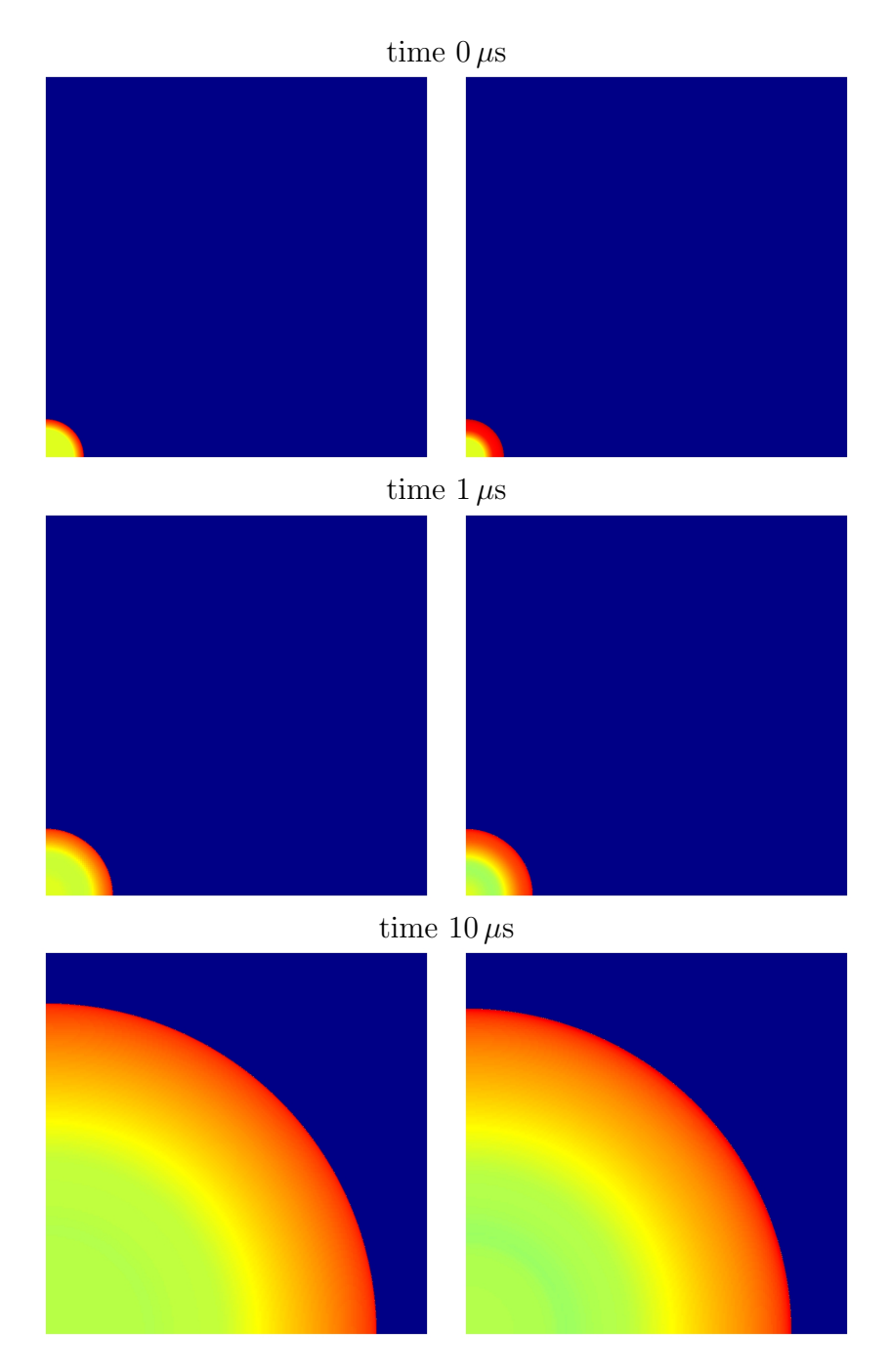


Figure 5: 2-D pressure plots at a sequence of times. Log scale from 0.5 (blue) to 50 (red) GPa. Left plots for SURF model and right plots for SURFplus.

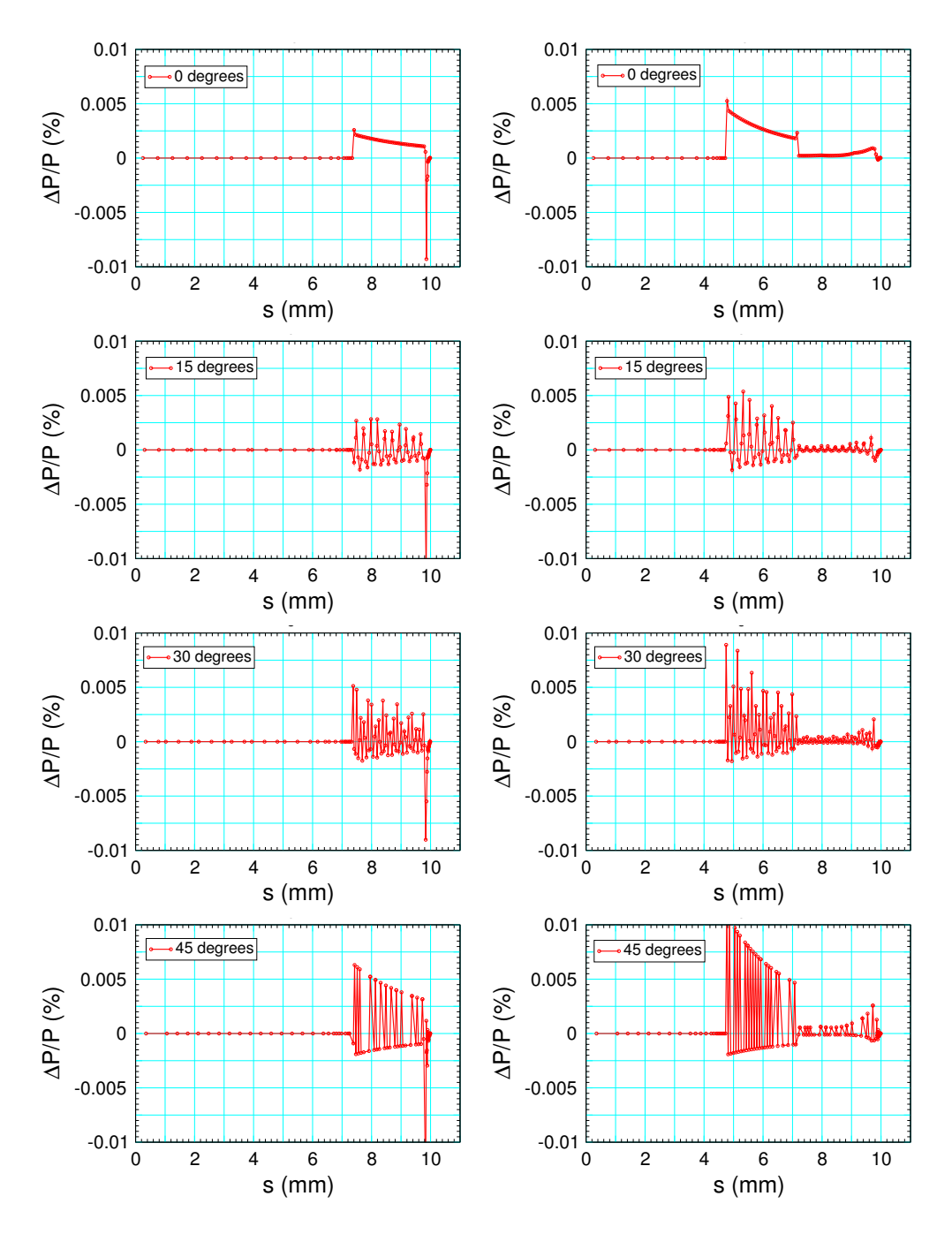


Figure 6: Pointwise error at t = 0 for pressure profiles along rays at angles 0, 15, 30, 45 degrees. Left plots for SURF model and right plots for SURFplus.

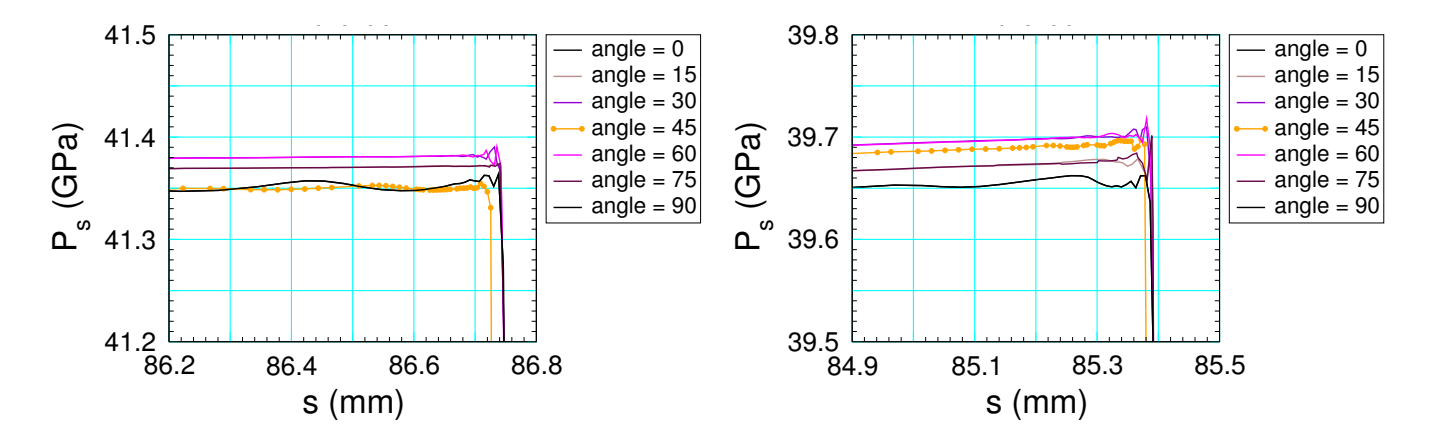


Figure 7: Detected shock pressure (advected) in the neighborhood of the detonation front at $t = 10 \,\mu s$. Left plot for SURF model and right plot for SURFplus. Symbols on 45 degree ray correspond to cells.

The angular dependence of the detected shock pressure near the detonation front at $t = 10 \,\mu s$ is shown in fig. 7. The variation with angle is small; 0.05 GPa compared to shock pressure of about 40 GPa. Due to the larger curvature effect for SURFplus, the shock pressure and the shock position for the SURFplus simulation are slightly lower than the corresponding values for the SURF simulation. We also note that the shock position at 45 degrees lags by 0.010 and 0.020 mm for SURF and SURFplus, respectively.

The angular dependence of the pressure profiles for the fast reaction zone at a select times is shown in fig. 8. The largest discrepancy is a small offset in the lead shock position of the 45 degree ray at late time. The offset was noted above in the detected shock pressure plot. A small difference also occurs in the profiles at the end of the reaction zone. This is due to smoothing of the pressure kink at the end of the reaction zone.

Pressure profiles and the pointwise error at a sequence of times for the SURF and SURFplus simulations are shown in fig. 9 and fig. 10, respectively. For the pointwise error, a small offset is used to align the 1- and 2-D detonation fronts. The offset is determined by minimizing the sum of the pointwise errors for first 20 points behind the lead shock front, which is taken to be the position of the maximum pressure.

The offset grows in time; from $0.036\,\mathrm{mm}$ at $t=1\,\mu\mathrm{s}$ to $0.146\,\mathrm{mm}$ at $t=10\,\mu\mathrm{s}$ for SURF, and from $0.022\,\mathrm{mm}$ at $t=1\,\mu\mathrm{s}$ to $0.079\,\mathrm{mm}$ at $t=10\,\mu\mathrm{s}$ for SURFplus. The effect is smaller for SURFplus than for SURF due to the larger reaction zone width from the slow second reaction. The increasing offset implies that the detonation speed is slow compared to the high resolution simulation. The effect is small, less than 0.2 per cent; about $0.14\,\mathrm{mm}/10\,\mu\mathrm{s}$ compared to planar detonation speed of $7.7\,\mathrm{mm}/\mu\mathrm{s}$. A slower detonation speed with increasing cell size has been observed before for simulations of the cylinder test; see [Menikoff, 2014].

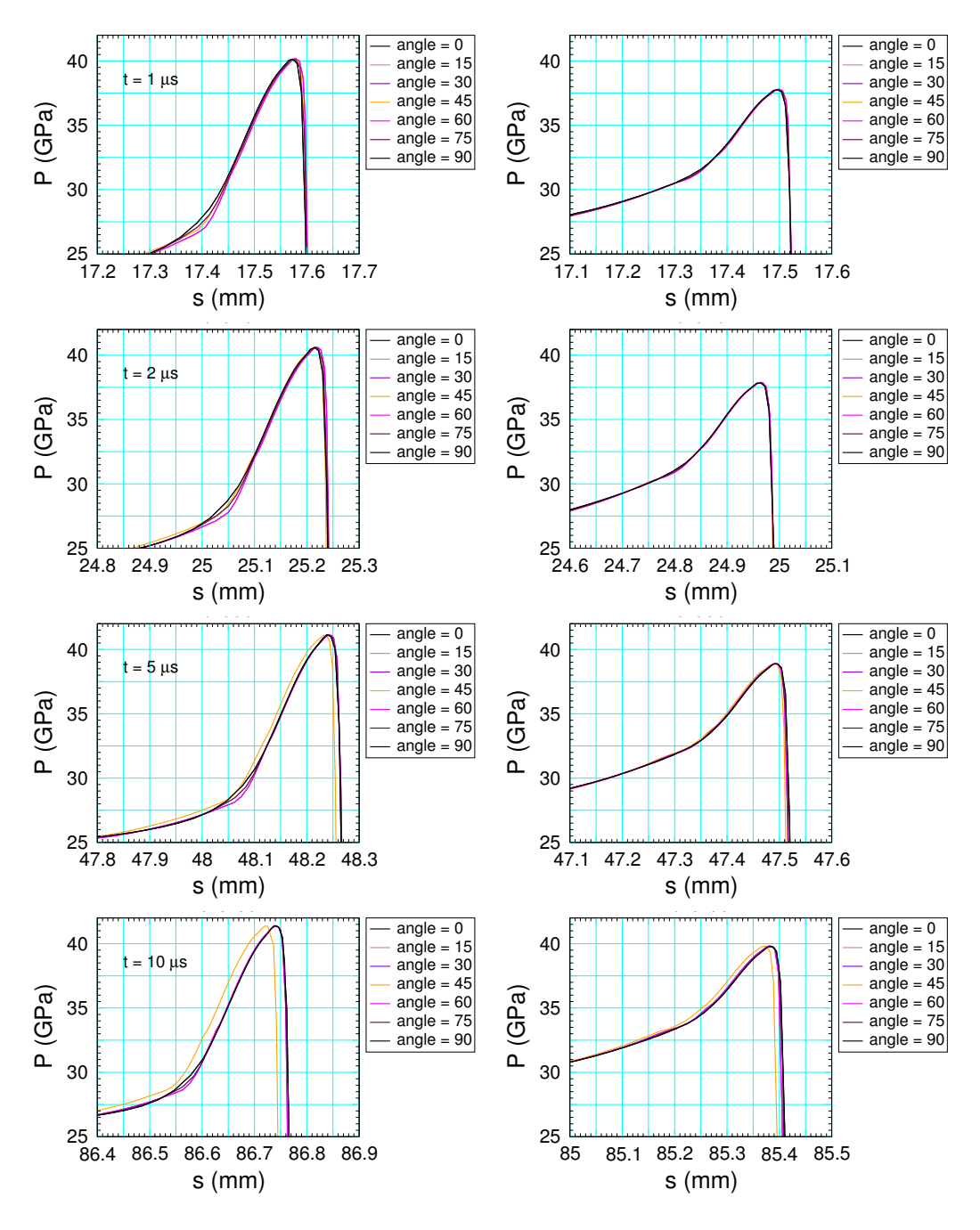


Figure 8: Angular dependence of fast reaction zone at selected times. Left plots for SURF model and right plots for SURFplus.

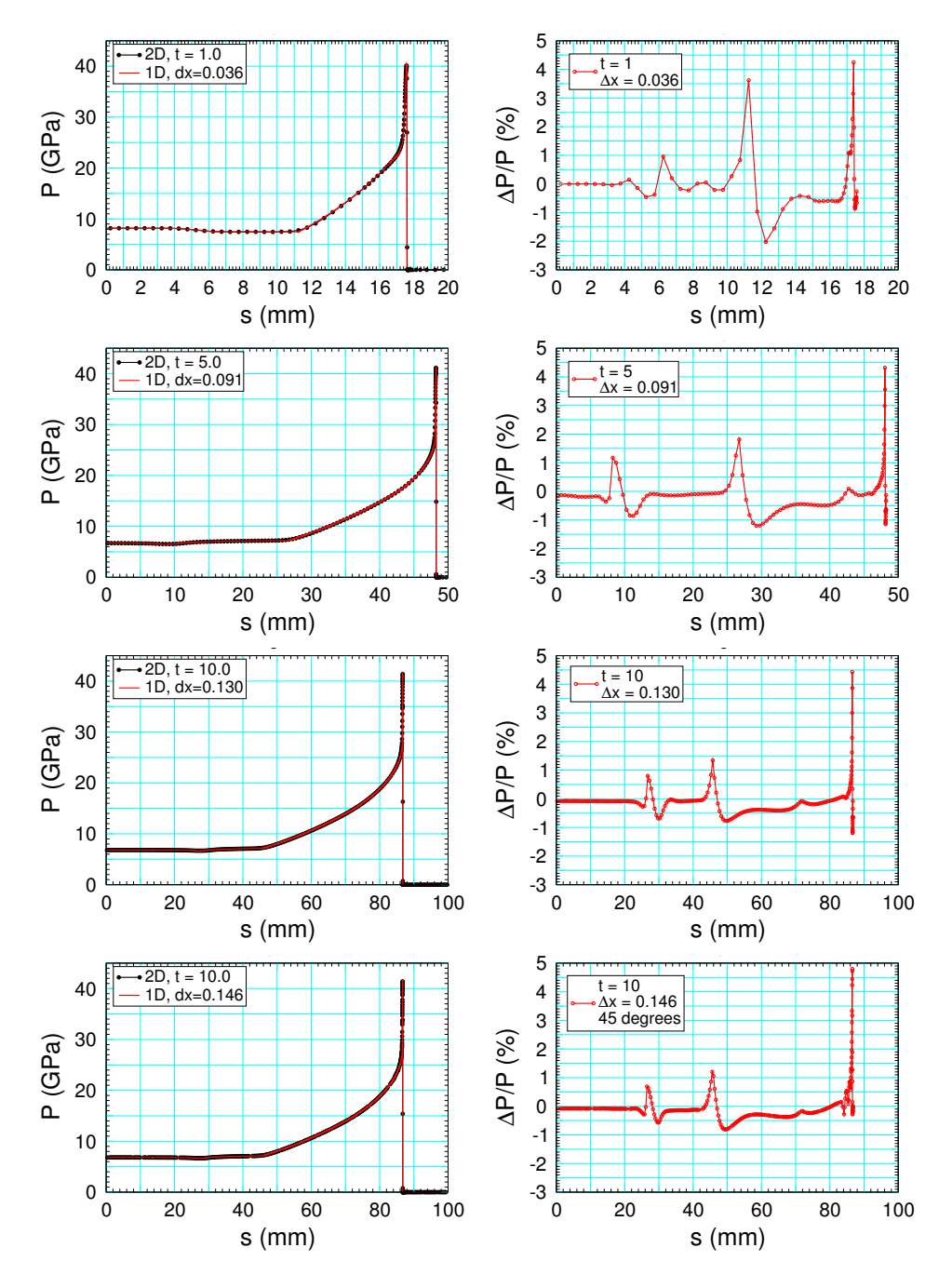


Figure 9: Pressure profile and pointwise error for SURF simulation. Left plots for pressure profile and right plots for pointwise error. Ray angle 0 unless specified in legend. Error is based on high resolution 1-D cylindrical simulation.

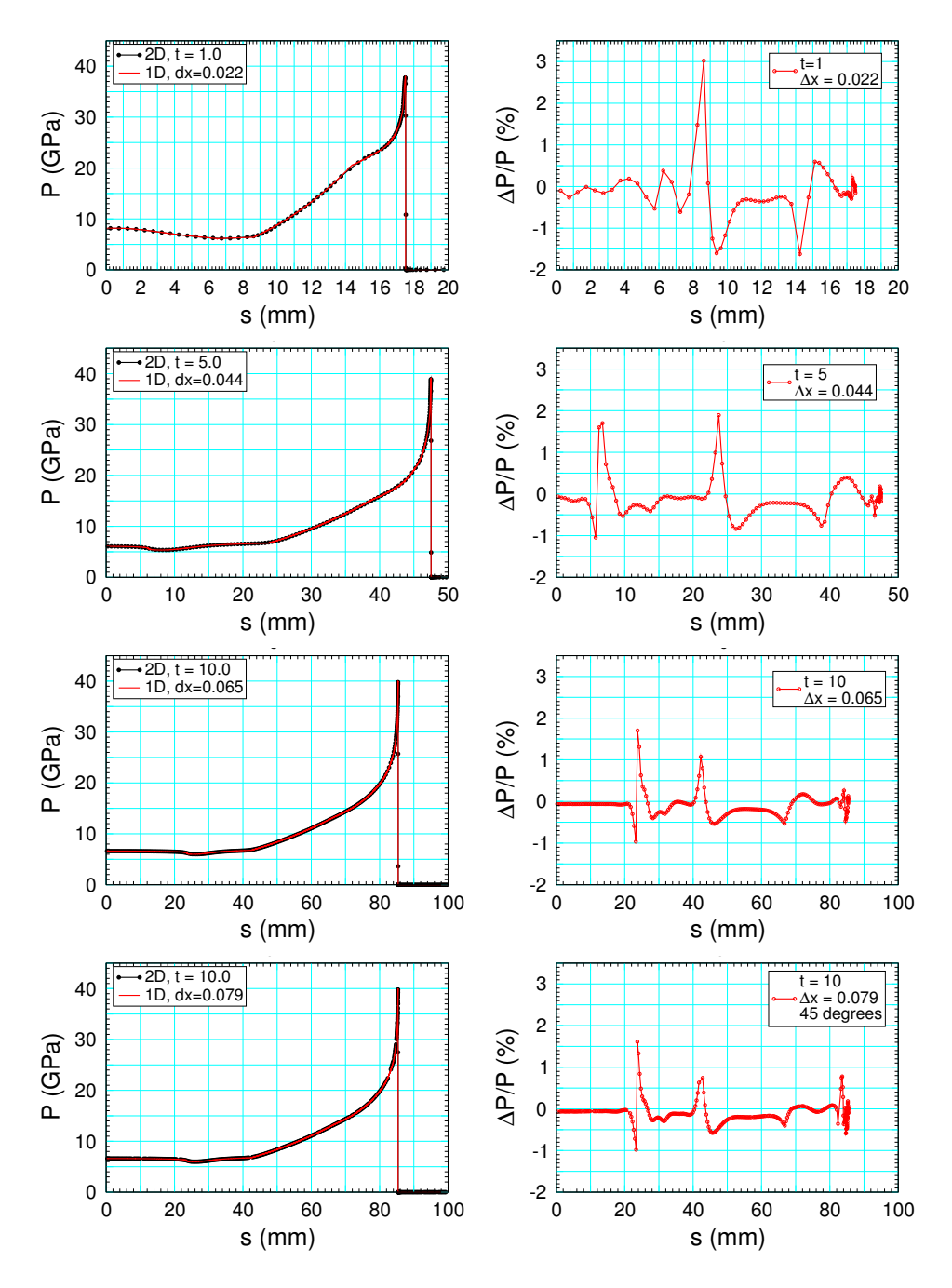


Figure 10: Pressure profile and pointwise error for SURFplus simulation. Left plots for pressure profile and right plots for pointwise error. Ray angle 0 unless specified in legend. Error is based on high resolution 1-D cylindrical simulation.

The plots of the pointwise error show several large peaks. We focus on the plots at the end of the run ($t = 10 \,\mu\text{s}$). The first peak at $s \approx 25 \,\text{mm}$ corresponds to the front of a weak outgoing shock generated at startup from the CJ release wave and geometric source terms. It shows up with the fine grid (cell size 7.8 μm) of the 1-D simulation but is smeared out with the coarse zoning (0.5 mm) of the 2-D AMR grid. The second peak at $s \approx 42 \,\text{mm}$ corresponds to the kink at the tail of the release wave. The large peak in the SURF simulation at $s = 86.5 \,\text{mm}$ corresponds to the kink at the end of the reaction zone. Due to the slow reaction in the SURFplus simulation, the kink at the end of the reaction zone is small and the prominent peak is absent. However, there is a reaction zone peak at early time ($t = 1 \,\mu\text{s}$) when the kink is larger. Aside from the prominent peaks noted above, the pointwise error is within $\pm \frac{1}{2}$ per cent.

4 Summary

Compared to the 1-D simulations of an underdriven detonation wave, the 2-D simulations of a cylindrically expanding detonation wave introduce two additional verification issues: cylindrical asymmetry due to alignment of detonation front with the computational grid, and time dependence of the detonation speed due to the curvature effect.

With an AMR grid having a cell size down to $7.8\,\mu\text{m}$, the error due to mesh alignment of the front is largest at 45 degrees. After $10\,\mu\text{s}$ or $75\,\text{mm}$ propagation distance, the azimuthal variation of the front position is small; $0.020\,\text{mm}$ compared to front radius of about $85\,\text{mm}$. The azimuthal variation of the detected shock pressure is also small; $0.05\,\text{GPa}$ compared to shock pressure of $40\,\text{GPa}$.

As with the 1-D simulations, for the pointwise error in the pressure profiles a small offset is used to align the simulated detonation front with the comparison solution. In 2-D the front offset grows in time. This implies the detonation speed is slightly low; about 0.2 per cent. A low detonation speed is compatible with the numerical curvature effect increasing with cell size. Aside from the prominent peaks at kinks in the pressure profile, the pointwise error is small; less than $\pm \frac{1}{2}$ per cent.

Differences between the SURF and SURFplus models result from the larger SURFplus reaction zone width due to the slow second reaction. In 2-D the larger reaction zone width results in a larger curvature effect. Consequently, at a fixed time, for the SURF simulation the detonation front is slightly ahead and the lead shock pressure is slightly higher than the corresponding values for the SURFplus simulation.

Overall, this and the previous two verification studies show that the SURF and SURFplus models in the xRage code propagate detonation waves in accordance with theory. Due to the small reaction zone width $(0.2 \, \text{mm})$ of the fast (PBX 9502) reaction, high resolution is needed

for an accurate solution; cell size less than $10 \,\mu\text{m}$, for pointwise error in release wave pressure profile of a few tenths of a per cent. Larger pointwise errors occur in the reaction zone and in the neighborhood of kinks in the pressure profile at the head and tail of the release wave. There is no indication of anything amiss in the implementation of the models.

References

- R. Menikoff. Effect of resolution on propagating detonation wave. Technical Report LA-UR-14-25140, Los Alamos National Laboratory, 2014. URL http://dx.doi.org/10.2172/1136940.
- R. Menikoff. Shock detector for SURF model. Technical Report LA-UR-16-20116, Los Alamos National Lab., 2016a. URL http://www.osti.gov/scitech/servlets/purl/1234496. 2
- R. Menikoff. Verification test of the SURF and SURFplus models in xRage. Technical Report LA-UR-16-23636, Los Alamos National Lab., 2016b. URL http://www.osti.gov/scitech/servlets/purl/1254247. 2
- R. Menikoff. Verification test of the SURF and SURFplus models in xRage: Part II. Technical Report LA-UR-16-24352, Los Alamos National Lab., 2016c. URL http://www.osti.gov/scitech/servlets/purl/1258358. 2
- R. Menikoff and M. S. Shaw. Reactive burn models and Ignition & Growth concept. *EPJ Web of Conferences*, 10, 2010. doi: 10.1051/epjconf/20101000003. URL http://www.epj-conferences.org/articles/epjconf/pdf/2010/09/epjconf_nmh2010_00003.pdf. 2
- R. Menikoff and M. S. Shaw. The SURF model and the curvature effect for PBX 9502. Combustion Theory And Modelling, pages 1140–1169, 2012. doi: 10.1080/13647830.2012.713994. 2, 4
- M. S. Shaw and R. Menikoff. Reactive burn model for shock initiation in a PBX: Scaling and separability based on the hot spot concept. In *Fourteenth Symposium (International) on Detonation*, 2010. 2